

**Electronic Supplementary Information for New Journal of
Chemistry**

**Efficient separation of crude oil-in-water emulsion based on robust
underwater superoleophobic titanium dioxide coated mesh**

Weimin Liu^a, Mengke Cui Wu^a Yongqian Shen^{*,b}, Peng Mu^a, Yaoxia
Yang^a, Jian Li^{*,a}

a Research Center of Gansu Military and Civilian Integration Advanced Structural Materials, College of Chemistry and Chemical Engineering, Northwest Normal University, Lanzhou 730070, P. R. China.

b State Key Laboratory of Advanced Processing and Recycling of Non-ferrous Metals, Key Laboratory of Nonferrous Metal alloys and Processing, Ministry of Education, School of Materials Science & Engineering, Lanzhou University of Technology, Lanzhou 730050, P. R. China. E-mail: syqch@163.com.

a* Corresponding author. Tel.: +86 931 7971533.

E-mail address: jianli83@126.com (J. Li).

b* Corresponding author. Tel.: + 86 931 2976688.

E-mail address: syqch@163.com (Y. Shen).

Supplementary figure

Fig. S1. (a, b) Stability tests of the various surfactant-stabilized oil-in-water emulsions including crude-oil-in-water emulsion, after one month, the emulsions are still stable without demulsification.

Fig. S2. The EDX spectrum of the TiO₂ coated meshes.

Fig. S3. High-resolution XPS C1s, O1s, P2p, Al2p and Ti2p narrow scans as a functional electron binding energy.

Fig. S4 Pore size distribution and average pore size of as-prepared CFCMs-2300.

Fig. S5 Schematic diagrams on (a) IECF, (b) IACP of the AP binder and the interaction forces between the AP binder and (c) nanoparticles or (d) substrates.

Fig. S6. The underwater kerosene CA of the AP coated mesh (a) and TiO₂ coated mesh without AP (b).

Fig. S7. Digital photographs showing the implementing processes to demonstrate the anti-fouling property of the TiO₂ coated mesh for the crude oil with high viscosity.

Fig. S8. The device for oil-in-water emulsion separation connected with a vacuum pump.

Fig. S9. The unmodified stainless steel cannot separate surfactant-stabilized oil-in-water emulsions.

Fig. S10. Optical microscope images and digital photographs of (a) hexane-in-water emulsion, (b) heptane-in-water emulsion and (c) petroleum ether-in-water emulsion before and after separation. Droplet size measurements of (d) hexane-in-water emulsion, (e) heptane-in-water emulsion and (f) petroleum ether-in-water emulsion

before and after separation.

Fig. S11. The schematic diagram of sand impact test.

Fig. S12. Variation in the underwater kerosene CAs of the TiO_2 coated mesh as a function of pH values.

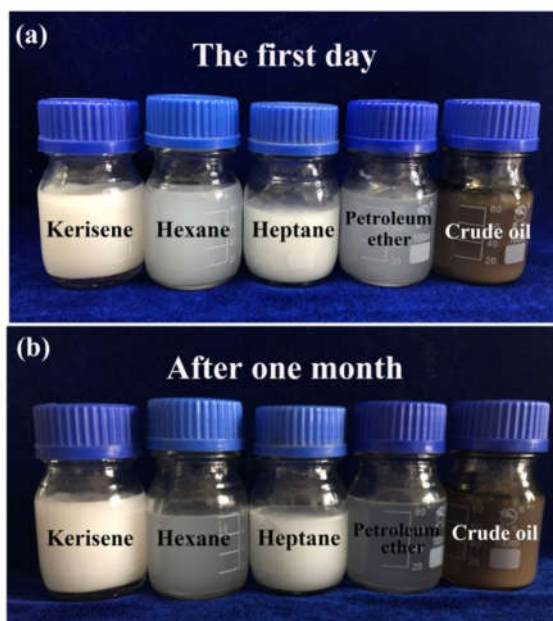


Fig. S1. (a, b) Stability tests of the various surfactant-stabilized oil-in-water emulsions including crude-oil-in-water emulsion, after one month, the emulsions are still stable without demulsification.

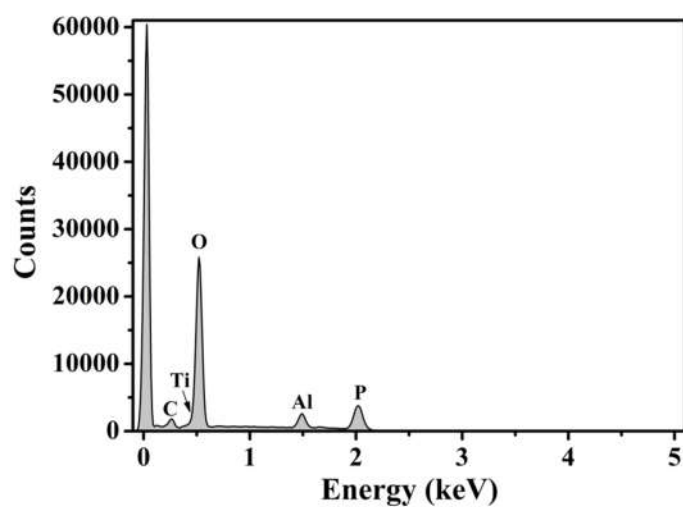


Fig. S2. The EDX spectrum of the TiO_2 coated meshes.

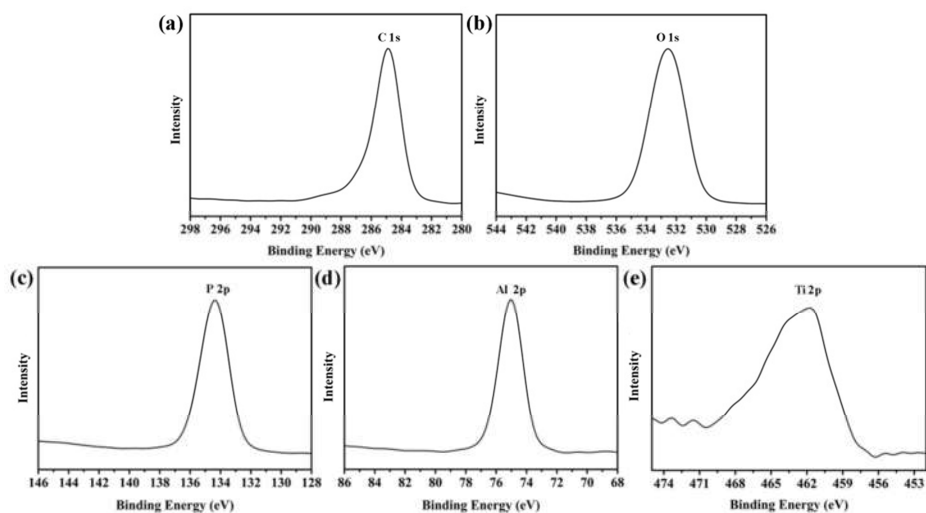


Fig. S3. High-resolution XPS C1s, O1s, P2p, Al2p and Ti2p narrow scans as a functional electron binding energy.

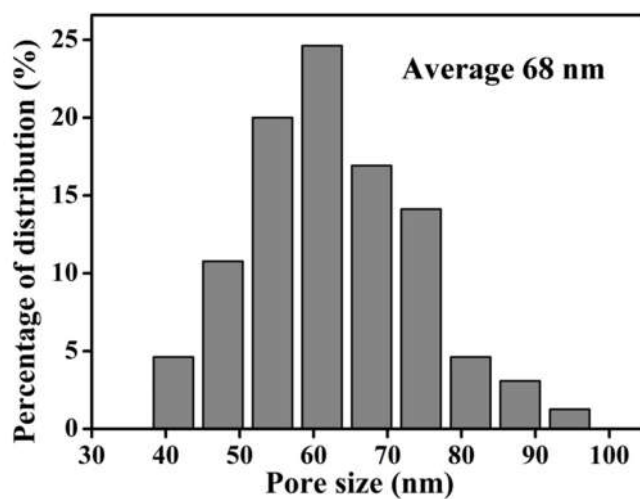


Fig. S4 Pore size distribution and average pore size of as-prepared CFCMs-2300.

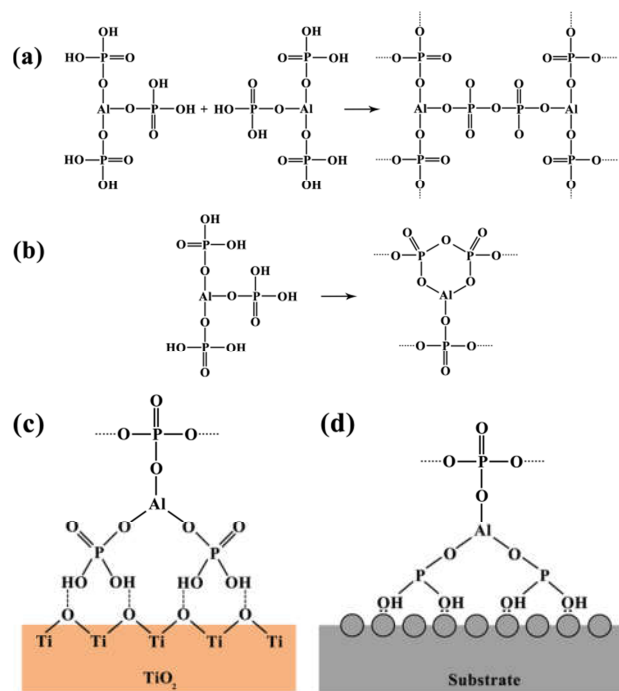


Fig. S5 Schematic diagrams on (a) IECP, (b) IACP of the AP binder and the interaction forces between the AP binder and (c) nanoparticles or (d) substrates.

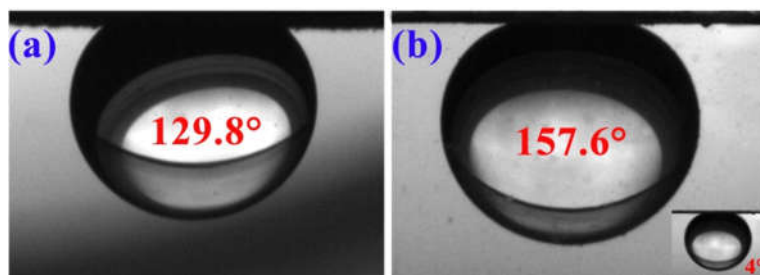


Fig. S6. The underwater kerosene CA of the AP coated mesh (a) and TiO_2 coated mesh without AP (b).

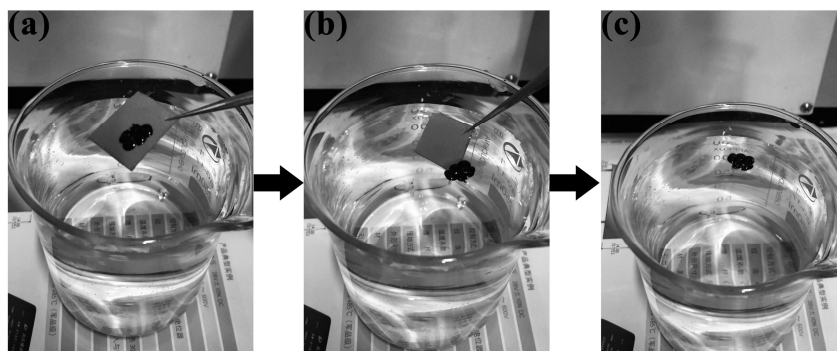


Fig. S7. Digital photographs showing the implementing processes to demonstrate the anti-fouling property of the TiO_2 coated mesh for the crude oil with high viscosity.

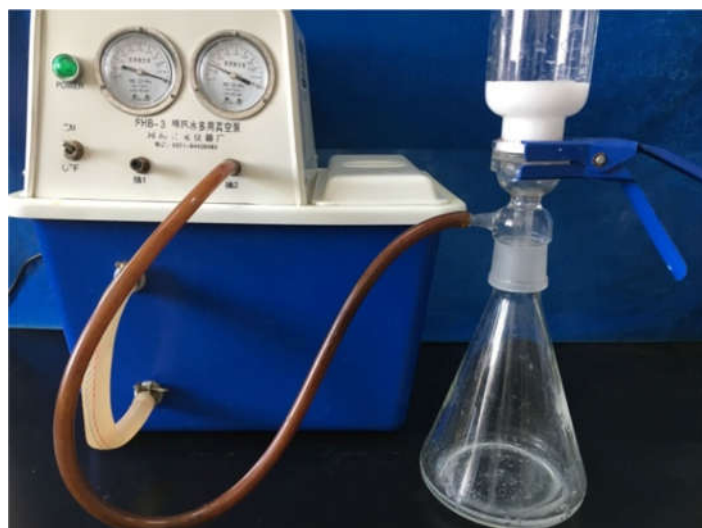


Fig. S8. The device for oil-in-water emulsion separation connected with a vacuum pump.



Fig. S9. The unmodified stainless steel cannot separate surfactant-stabilized oil-in-water emulsions.

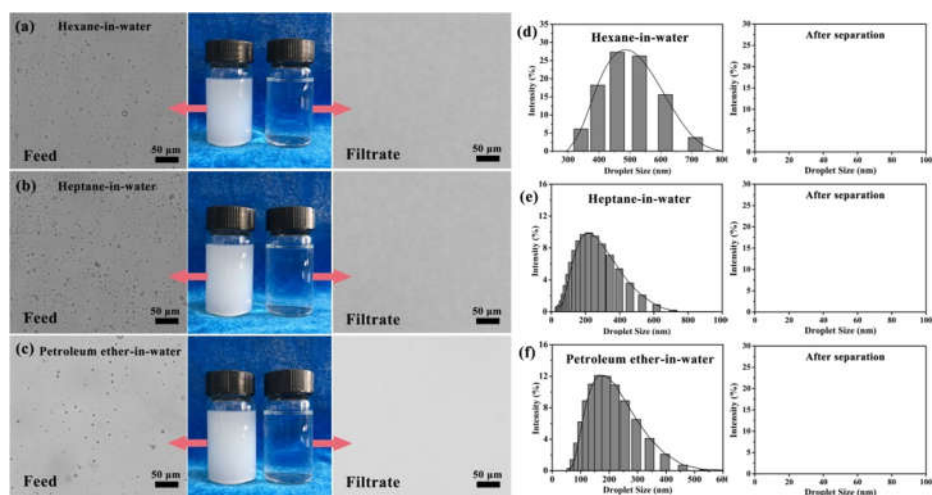


Fig. S10. Optical microscope images and digital photographs of (a) hexane-in-water emulsion, (b) heptane-in-water emulsion and (c) petroleum ether-in-water emulsion before and after separation. Droplet size measurements of (d) hexane-in-water emulsion, (e) heptane-in-water emulsion and (f) petroleum ether-in-water emulsion before and after separation.

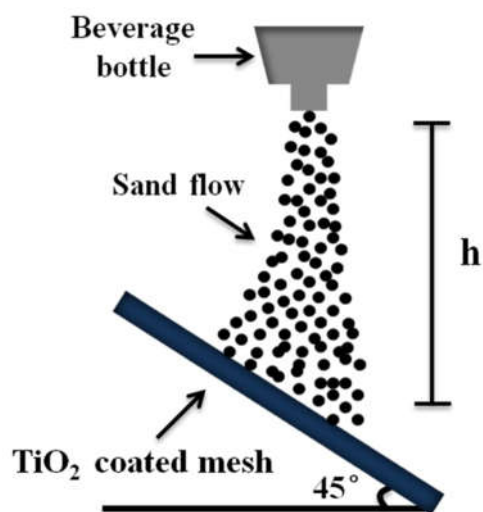


Fig. S11. The schematic diagram of sand impact test.

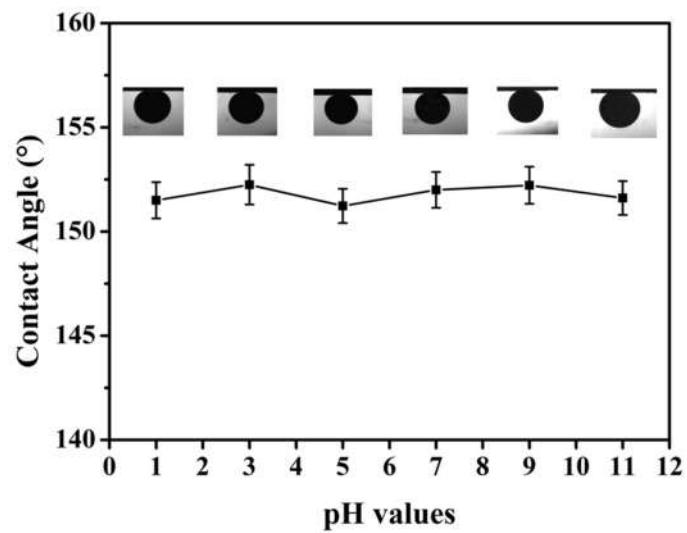


Fig. S12. Variation in the underwater crude oil CAs of the TiO_2 coated mesh as a function of pH values.